electronics

MDPI

Article

A Wireless Intelligent Motion Correction System for Skating Monitoring Based on a Triboelectric Nanogenerator

Zhuo Lu [1], Yuzhang Wen [2], Xu Yang [3], Dan Li [4], Bocong Liu [1], Yaotian Zhang [1], Jiabin Zhu [5], Yongsheng Zhu [2,*], Shouwei Zhang [1,*] and Yupeng Mao [1,2,6,*]

1 School of Physical Education, Northeast Normal University, Changchun 130024, China
2 Physical Education Department, Northeastern University, Shenyang 110819, China
3 Basic Department, Changchun Polytechnic, Changchun 130022, China
4 Physical Education College, Jilin University, Changchun 130012, China
5 Winter Olympic College, Harbin Sport University, Harbin 150008, China
6 School of Strength and Conditioning Training, Beijing Sport University, Beijing 100084, China
* Correspondence: 2001276@stu.neu.edu.cn (Y.Z.); zhangsw178@nenu.edu.cn (S.Z.); maoyupeng@pe.neu.edu.cn (Y.M.)

Abstract: Smart sport and big data have become inextricably linked with new technologies and devices to monitor sport-related information in real time. In this paper, a lightweight, portable and self-powered triboelectric nanogenerator (LPS-TENG) has been developed to monitor the frequency and force of skaters' pedaling. Friction layers are formed of polytetrafluoroethylene (PTFE) and nylon films. Based on the triboelectric effect, LPS-TENG does not require an external power supply, and it can be used to monitor biomechanical motion independently. Under the conditions of 1 Hz and 17.19 N, the outputting voltage of LPS-TENG is stabilized at 14 V. Wireless data transmission is achieved with the help of the LPS-TENG and AD module. Visual feedback is provided by the upper computer system in the process of processing data. The wireless intelligent motion correction system is composed of an LPS-TENG, an AD module and a back-end computer. It can clearly analyze the changes between different frequencies and forces during skating. Results showed that the signal of tester's high-frequency and great-force motion, was transmitted to the computer, and its feedback was given after analysis and processing successfully. The system may help coaches develop training methods, means and tactics to increase athletes' performance and competitive level in athletic sport. The purpose of this study is to provide new ideas for monitoring skaters' sport techniques, promote the use of force sensors in the monitoring of sport and develop intelligent assistant training systems.

Keywords: triboelectric; sports monitoring; self-powered; wireless transmission

Citation: Lu, Z.; Wen, Y.; Yang, X.; Li, D.; Liu, B.; Zhang, Y.; Zhu, J.; Zhu, Y.; Zhang, S.; Mao, Y. A Wireless Intelligent Motion Correction System for Skating Monitoring Based on a Triboelectric Nanogenerator. *Electronics* **2023**, *12*, 320. https://doi.org/10.3390/electronics12020320

Academic Editor: Min-Hsin Yeh

Received: 20 December 2022
Revised: 5 January 2023
Accepted: 5 January 2023
Published: 8 January 2023

1. Introduction

The Beijing Winter Olympics has provided a new impetus for the development of ice sports [1]. Speed skating is highly regarded because of its high-intensity competitive performance [2]. Considering that it has become increasingly difficult for professional speed skaters to improve their athletic performance [3], it is necessary to resort to relevant scientific tools in training [4,5], which are essential to improve the quality of athletes' training. The force and frequency of the athlete's pedaling have a great impact on the athlete's performance [6], and effective monitoring is very important to improve their performance [7]. However, traditional monitoring means mak it difficult to monitor the changes of the athletes' pedaling force and frequency in real-time [8], which means that the training and sports monitoring cannot be synchronized, and the training efficiency and pace slows down. At the same time, traditional monitoring means are not able to express the required motion data quantitatively. For example, morning pulse assessment [9], camera filming [10] and monitoring heart rate index, etc. are not conducive to real-time and refined training [11]. In addition, traditional testing equipment is heavy in mass, less flexible and not portable enough to use [12–14]. In order to build the required database for athletes, a lot of analysis and calculations must be performed, which greatly increases the cost of purchasing and maintaining the equipment [15,16]. When commercial sensors are used for monitoring, the durability of battery also becomes an obstacle to its further application [17–20]. Piezoelectric has the advantages of being flexible and portable [21], but it is difficult to manufacture the piezoelectric film [22]. Therefore, it is necessary to develop a portable, self-powered and durable sensing device to monitor athletes' skating process to enhance training rhythm and speed and further improve training quality.

Academic Zhonglin Wang successfully developed the triboelectric nanogenerator (TENG) in 2012 [23–26]. TENG is a new type of energy-harvesting technology which can collect signals such as acceleration and pressure in the irregular low-frequency human body [27,28]. As a sensor, it can be designed with thin-layer electrodes to achieve the effective output of current. TENG is inexpensive, simple, self-powered and available in a wide range of materials compared to conventional sensors [29–31], and these advantages are very important for sensors. At the same time, interdisciplinary cooperation is more conducive to the development and innovation of sports [32]. TENG has good application prospects in the field of intelligent sports, and it will become a new technology for sports monitoring [33–36]. In addition, the force sensor based on TENG has been able to achieve various applications such as gait recognition [37,38], monitoring the comfort of sports shoes [39] and restoring the human body's sense of touch [40,41], etc. The application of force sensors in these areas has certain significance for research in the field of sports monitoring.

This paper presents a lightweight, portable and self-powered triboelectric nanogenerator (LPS-TENG) as a skating monitoring sensor. It is installed on the back of the heel of the Klap skates to monitor the motion frequency and force of the athletes. The sensor consists of a common copper sheet as the electrode, polytetrafluoroethylene (PTFE) and nylon as the friction layer, and the substrate is made by 3D printing. The LPS-TENG is cost effective in material, lightweight and portable. The voltage signal is generated by body motion and wirelessly transmits the generated voltage signal through an AD module to monitor athletes' motion in real time. In addition, we designed a wireless intelligent motion correction system that can monitor the frequency and force of the pedaling and give feedback. This system can help coaches to optimize athletes' starting and sprinting techniques, formulate correct training methods and means and thus improve athletes' sports performance and competitive level. This work aims at providing new ideas for monitoring skaters' sports techniques, promoting the application force sensors in the field of sports monitoring and promoting the development of intelligent assistant training systems.

2. Materials and Methods

2.1. Materials

PTFE film (0.03 mm) was purchased from Taobao. Polyamide-66 (PA-66) film was purchased from Dongguan Yixuan Plastic Co, Ltd. (Dongguan, China). The substrate was fabricated by a 3D printer. The model of the 3D printer is JGAURORA-A6. Polylactic acid (PLA) is the 3D printing material. The parameters of the 3D printer are as follows: the layer height is 0.1 mm; the thickness of shell is 1.2mm; the packed density is 100%; the printing temperature is 200 degrees Celsius; the hot bed temperature is 50 degrees Celsius and the printing speed is 50 mm/s. The 3D substrate with a radius of 0.5 mm is printed for 15 min.

2.2. Method

Firstly, a cylindrical substrate was made by 3D printer. Secondly, PTFE film, nylon film and copper foil were cut into appropriate size circles. Finally, PTFE film, nylon film and copper foil were pasted on the surface of the cylindrical substrate.

2.3. Testing

An oscilloscope (sto1102c, micsig) made in China was used to test the LPS-TENG output performance and practical applications. The output performance of the device was tested using a stepper motor. In the actual test, the LPS-TENG was installed on the back of the heel of the Klap skates and the performance was tested. In addition, a wireless data acquisition module was designed, and the integration of the LPS-TENG and the wireless AD module enables the wireless transmission of signals. The principle of the AD module is that the AD module converts the electric signal into a digital signal. Then, the Bluetooth transmits the digital signal to the receiver module. Finally, the computer displays the results. The chip of the AD module is stm32 and the model of Bluetooth is HC-05. The actual picture of the AD module is shown in Figure S1, and the circuit diagram of the AD module is shown in Figure S2.

3. Results

In this paper, a self-powered sensor is designed to monitor the frequency and force of skating in real-time. Based on the output of the signal, coaches can understand and observe the dynamic changes of athletic performance during training and competition in real-time, so as to find out the problems existing in the training and help athletes improve the training effect and sports performance. A schematic of the self-powered sensor used to monitor skating technology and collect motion data is shown in Figure 1. Figure 1a shows a schematic of the pedaling force and frequency of skating. We can obtain the sports data during the skating process by monitoring the Klap skates. The LPS-TENG converts the mechanical movement of the human body into electrical signals which enter the computer through wireless transmission. Through analysis of the electronic signal, we learned the information of the pedaling frequency and force in the skating process. Klap skates were selected due to their unique characteristics. Klap skates are unique in that the front bracket of the skates is connected to the skates through hinges, and the rear bracket can be separated from the skates at any time. The self-powered sensor (r = 5 mm) is integrated into the heel of the Klap skates; it can monitor changes in the skater's motion parameters, such as frequency and force, in real-time. In this process, the sensors work without the support of an external power source and are able to transmit wirelessly to build sports data. Coaches and athletes use this data for technical and tactical analysis and development, providing more possibilities for sports monitoring. Figure 1b shows the optical image of the sensor and the 3D structure of the device. The sensor, having light weight, light volume and no damage to the original structure of skates can minimize the interference to athletes. Therefore, nylon and PTFE are used as friction layers of sensors because of their excellent sensing performance, and copper foils on the upper and lower sides are used as electrodes. Figure 1c is the system block diagram of the sensor work. Firstly, the sensor collects the biomechanical energy, converts it into an electrical signal and outputs it in the form of alternating current. Secondly, the sensor accomplishes wireless data transmission through the AD module. Finally, coaches monitor and analyze athletes' training data in real-time.

The detailed working mechanism of the sensor and the potential distribution during operation COMSOL simulation are shown in Figure 2. Figure 2a shows the working mechanism of the LPS-TENG. The vertical contact separation mode is adopted. At stage I, the athletes are in a standing position. Under the influence of the athlete's gravity, the two friction layers contact each other, and the surfaces of the two friction layers produce equal and opposite induced charges. At stage II, when the athletes pedal, the two friction layers begin to separate. A small distance is generated between the friction layers and an induced potential difference is generated between the two electrodes. Electrons flow from the PTFE to the nylon, resulting in a downward current. At stage III, the pedal action is finished, the two friction layers are completely separated, and the electrostatic field is balanced. At stage IV, due to the influence of the rebound force of the Klap skates, the two friction layers are close. The electrons return, producing an upward current. When the upper and lower friction layers fully contact, a cycle is completed. In order to further understand the working mechanism of the LPS-TENG, a simulation of potential distribution was performed in COMSOL software (Figure 2b). The potential difference between the upper and lower electrodes changes with the change of the friction layer distance, showing an increasing trend.

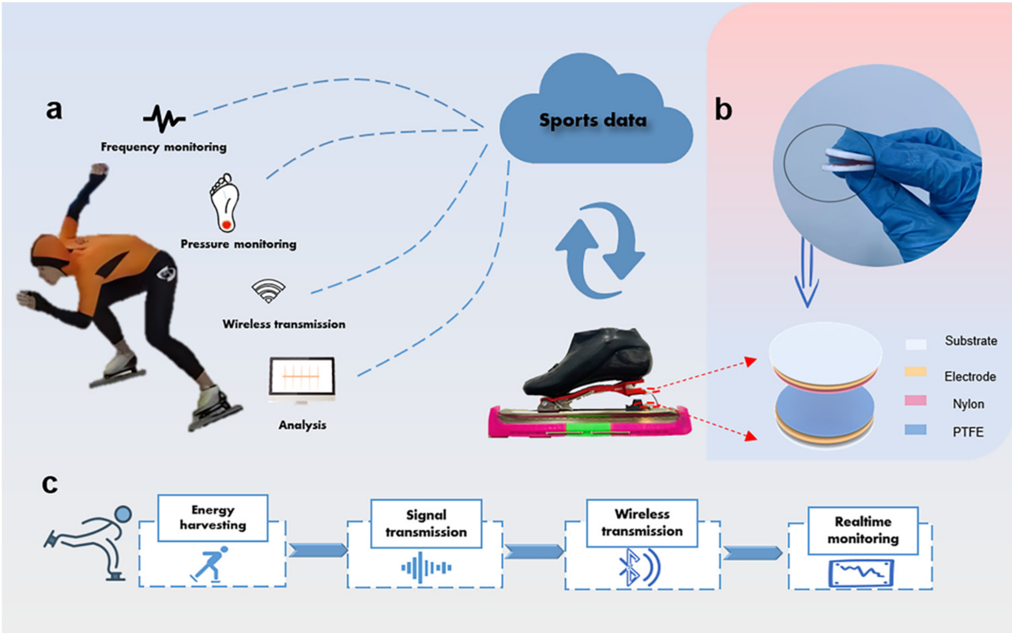

Figure 1. Experimental design of a self-powered motion sensor for skating technology monitoring. (**a**) Schematic diagram for monitoring frequency and force of skating pedaling. (**b**) Optical image and structure of the sensor. (**c**) Block diagram of the system showing energy collection, signal transmission and wireless monitoring.

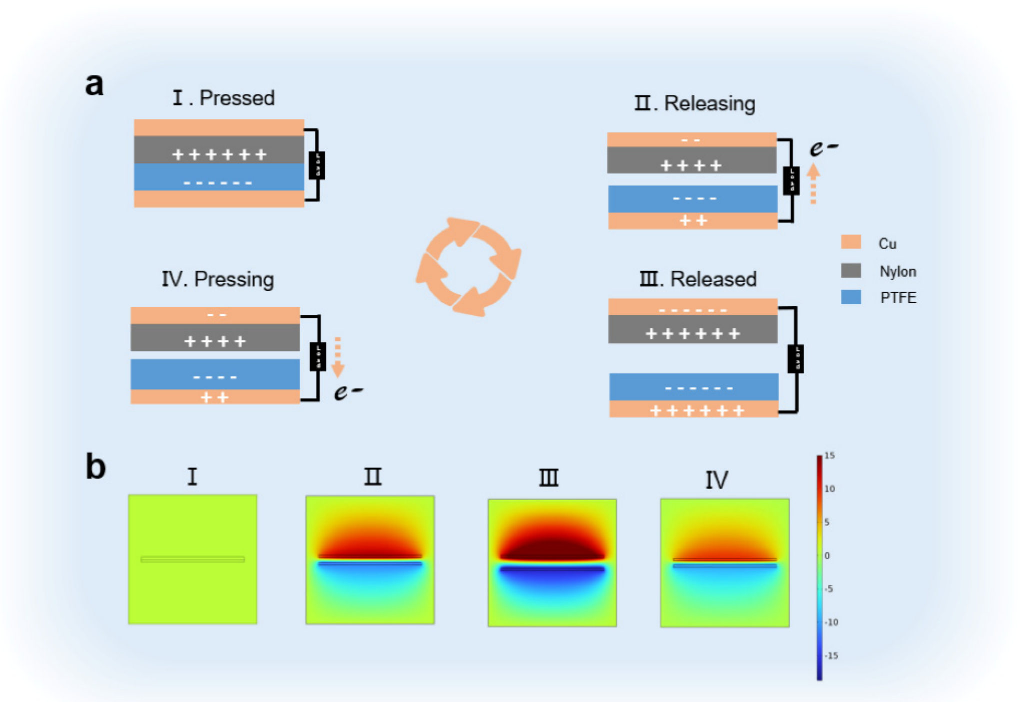

Figure 2. The LPS-TENG working mechanism and COMSOL potential distribution simulation. (**a**) Schematic diagram of the working mechanism of the LPS-TENG. (**b**) COMSOL simulation of the potential distribution of the LPS-TENG.

The selection of materials plays a pioneering role in the process of making sensor devices [42,43]. The output performance of the LPS-TENG demonstrated under different experimental conditions is shown in Figure 3. Figure 3a demonstrates the output performance of various different friction layer materials. The voltage generated by the combination of nylon and PTFE can reach 28.65 V, which is superior to other materials. Therefore, nylon and PTFE are used as triboelectric materials for the LPS-TENG. Excellent electrical performance is an important index of sensor devices [44]. Figure 3b shows the output voltage of the LPS-TENG at different frequencies. When testing frequency, we tested 77 sets of data. When the frequency is 0.5 Hz, 1 Hz, 1.5 Hz, and 2 Hz, respectively, the average output voltages are 11.88 V, 11 V, 12.61 V, and 12.03 V. It can be seen that the output voltage of the LPS-TENG is basically constant at different frequencies. The blue line is the linear fit (Figure S3) and the linear fit of Equation (1) is as follows:

$$\mathrm{V} = 11.36 + 0.41 \times \mathrm{Hz} \tag{1}$$

where V represents the output voltage (V) and Hz represents the pedaling frequency (Hz). The linearity value of 0.39936 is a weak correlation. Figure 3c shows the relationship between frequency and output voltage. The device response can be calculated by the following Equation (2):

$$\mathrm{R}\% = \left| \frac{\mathrm{V_0} - \mathrm{V_i}}{\mathrm{V_0}} \right| \times 100\% \tag{2}$$

where V_0 represents the output voltage at 0.5 Hz and V_i represents the output voltage at an other frequency. When the LPS-TENG works at 0.5 Hz, 1 Hz, 1.5 Hz and 2 Hz under fixed force, the corresponding output voltage response is 0%, 8%, 5.8% and 1.2%, respectively. It shows that the output voltage of the LPS-TENG hardly changes with the motion frequency. From the above results, it can be concluded that the output frequency of voltage increases with the increase in pedaling frequency, so the LPS-TENG can be used to monitor the change of pedaling frequency during skating. By monitoring the speed of the pedaling frequency of skating, coaches can know the weak points of athletes' sports skills and can reasonably arrange their skills and tactics in skating competitions. Figure 3d shows the output voltage of the LPS-TENG at different forces (1 Hz). When testing force, we tested 100 sets of data. When the force is 16.03 N, 20.14 N, 27.9 N, and 34.29 N, the LPS-TENG's average output voltage is 13.24 V, 16.42 V, 21.5 V, and 27.96 V, respectively. It can be seen that under different forces, the output voltage of the LPS-TENG increases with the increase in force. The red line is the linear fit (Figure S4), and the linear fit of Equation (3) is as follows:

$$\mathrm{V} = 0.42 + 0.79 \times \mathrm{N} \tag{3}$$

where V represents the output voltage (V) and N represents the pedal force (N). The linearity value reached 0.99539 with a strong correlation. Figure 3e shows the relationship between force and output voltage. It can be seen that the higher the force, the higher output voltage. Additionally, the LPS-TENG output voltage response is proportional to force. V_0 represents the voltage at a force of 16.03 N, and V_i represents the voltage at another force. The response of the LPS-TENG under 16.03 N, 20.14 N, 27.90 N and 34.29 N force corresponds to 0%, 24%, 38% and 53%. From the above results, it can be concluded that the output voltage increases with the force, so the LPS-TENG can be used to monitor change of pedaling force during the skating motion. Figure 3f–g shows the changes of voltage, current and power of the sensor at different resistances. We use external resistance to calculate the current [45]. When the resistance increases, the voltage increases and the current decreases. The power reaches its maximum value when the resistance is 6 MΩ. The maximum voltage, current and power is 0.934 V, 0.178 μA and 0.088 μW, respectively. Figure 3h,i shows the durability test of the LPS-TENG after 1400 s of continuous operation. From the figure, it can be concluded that the output voltage of the LPS-TENG can be stabilized at 14 V after 1400 s of continuous operation. The results show that the LPS-TENG can be used to monitor the athletes' motion information during the skating routine training.

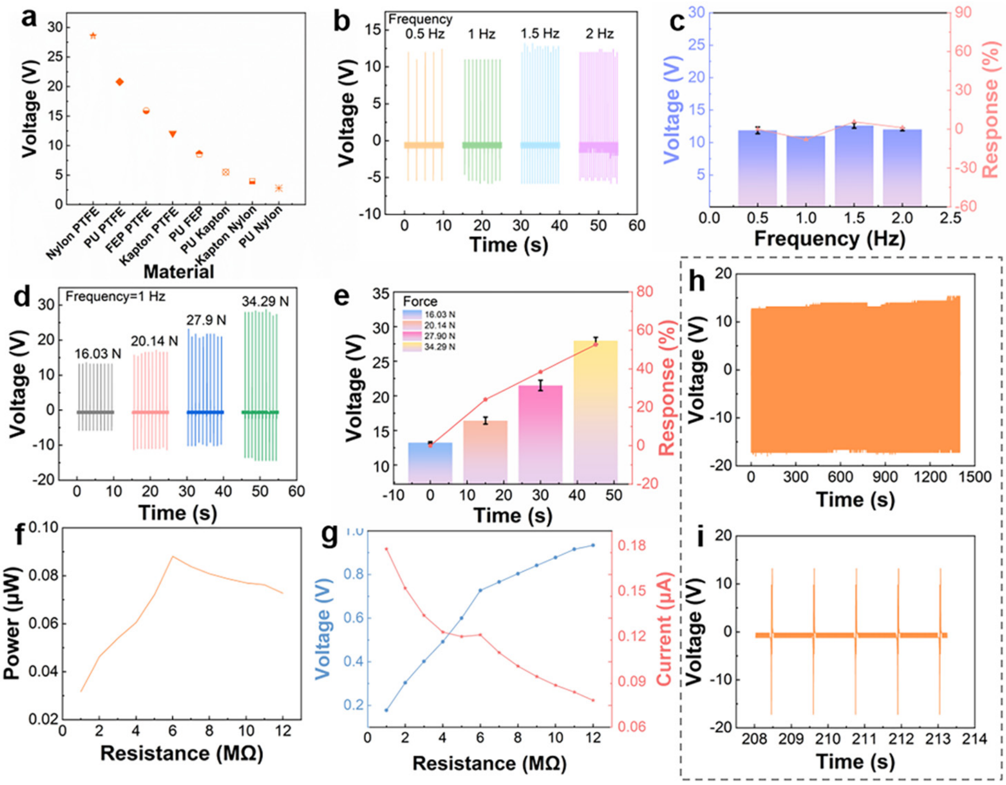

Figure 3. Output voltage performance of the LPS-TENG. (**a**) Output voltage combined with different materials. (**b**) Output voltage of the LPS-TENG at different frequencies. (**c**) Output voltage and response of the LPS-TENG at different frequencies. (**d**) Output voltage of the LPS-TENG at different forces. (**e**) Output voltage and response of the LPS-TENG at different forces. (**f**) Power of the LPS-TENG at different load resistances. (**g**) Output voltage and output current of the LPS-TENG at different load resistances. (**h**) Durability test of the LPS-TENG. (**i**) Endurance details.

In sports monitoring, wireless transmission of sports data can minimize the interference of sensors on athletes' training [46]. The combination of the LPS-TENG and AD module can accomplish this very well. Additionally, the AD module circuit is shown in Figure S1. The LPS-TENG signal wireless transmission system is shown in Figure 4a. The data information of the athletes' pedaling frequency and force are transmitted in real-time by the AD module, and the training data is analyzed and presented by the computer to provide a reference for the coaches. Figure 4b shows the voltage signal generated by the LPS-TENG in real-time when the tester is exercising. The computer terminal displays the sensing signal (Video S1) in real-time when the athlete performs a stroking motion. The signals generated by the LPS-TENG correspond to the frequency and force of pedaling accurately, which is convenient for real-time monitoring of athletes. Figure 4c–g shows the normalized voltage generated by the LPS-TENG under different pedaling frequencies and forces. Figure 4d shows the normalized voltage obtained by the tester at low-frequency motion with different pedaling forces. From the graph it can be seen that at lower frequency, the LPS-TENG can clearly monitor the force of the pedaling. Figure 4e shows the normalized voltages obtained with different pedaling forces at high-frequency motion. Under the condition of high frequency, the change of pedaling force can also be clearly monitored by the LPS-TENG. Although there is a slight difference between the frequencies in Figure 4d,e, from the perspective of human movement, this slight difference will determine whether one can win the competition or not [47]. The comparison of Figure 4d,e shows that the LPS-TENG can collect data for different pedaling forces at different pedaling frequencies. Figure 4f shows the normalized voltage for different pedaling frequencies at small pedaling forces, and the graph shows that the LPS-TENG can clearly monitor the change in frequency at small force. Figure 4g shows the normalized voltage for different pedaling frequencies at great pedaling forces. Under the condition of great pedaling force, the speed of frequency can also be clearly monitored by the LPS-TENG. In comparing Figure 4f,g, it can be seen that the LPS-TENG can collect the motion data of different pedaling frequencies under different pedaling force conditions of the tester. To sum up, the LPS-TENG can clearly analyze the changes between different frequencies and forces during athletes' motion. The data sports information enables motion intensity to be quantified. The coaches can detect the athletes' fatigue in a timely manner, adjust the training plan in time and reduce the motion intensity. Therefore, the LPS-TENG can be applied to the daily training of skaters, assisting coaches to analyze and make decisions on technical and tactical levels.

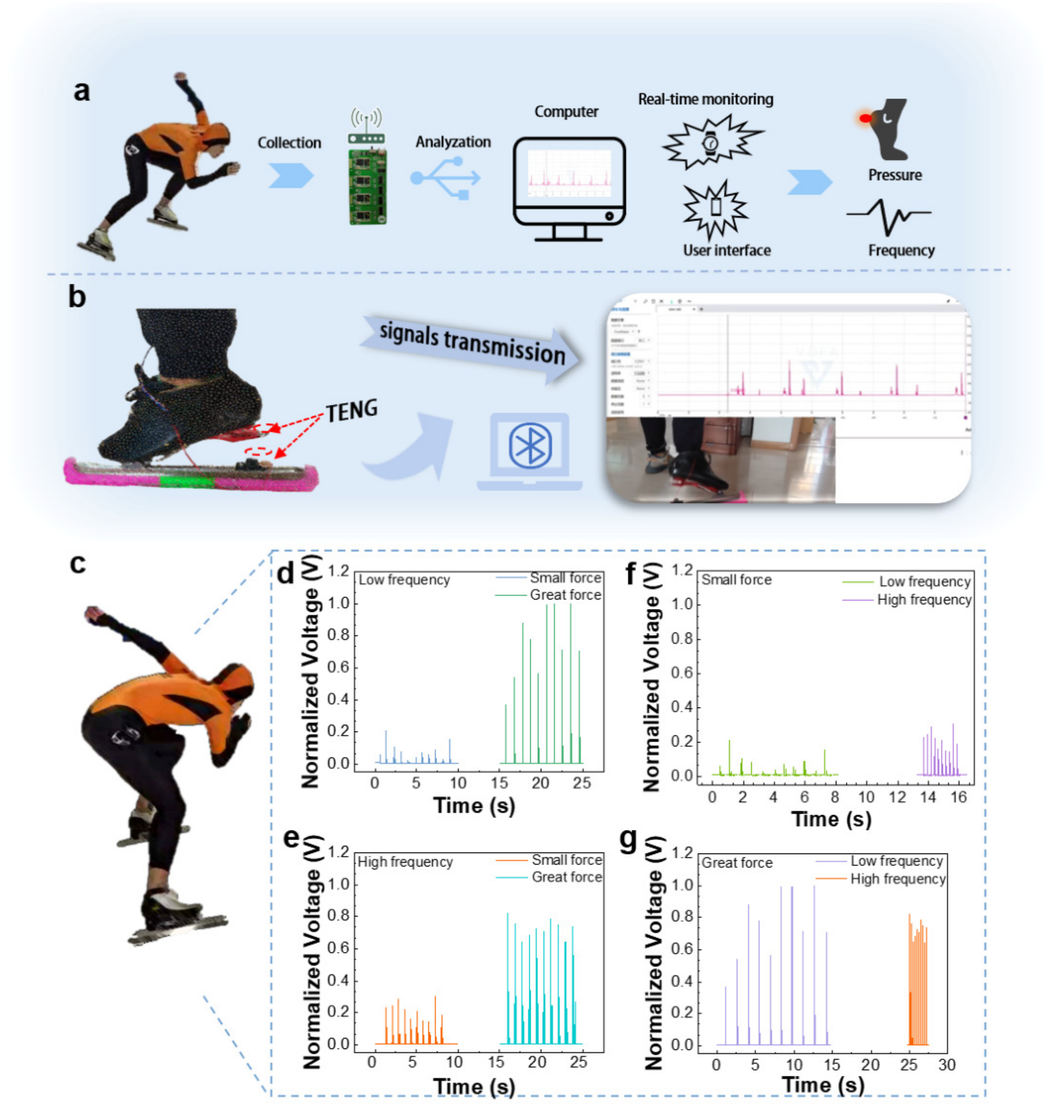

Figure 4. Actual test of the LPS-TENG signal wireless transmission system. (**a**) The working process of the wireless transmission system of the LPS-TENG signal. (**b**) The LPS-TENG generates voltage signal in real-time when the tester is exercising. (**c**–**g**) Normalized voltage generated by the LPS-TENG under different pedaling frequencies and pedaling forces.

In order to better monitor the pedaling frequency and force to assist athletes' training, a wireless intelligent motion correction system based on the LPS-TENG is designed in this paper. Figure 5a shows the workflow of the wireless intelligent motion correction system. The LPS-TENG wirelessly transmits the voltage signal to the computer through AD module. The computer analyzes and presents the data in real-time and gives feedback to the analysis and processing of athletes' pedaling frequency and force. Figure 5b shows the specific process of wireless intelligent motion correction system. Here, we use fast Fourier transform. When the signal is input, the frequency and amplitude are accurately transformed; this can accomplish the recognition of people. The upper computer acquires and processes the data, visualizes the presentation and provides real-time feedback (Video S2). When the tester is performing high-frequency and great-force motion, the signal is transmitted to the computer, which is analyzed and processed to produce successful feedback. When the tester is performing low-frequency and small-force motion, the signal is transmitted to the computer, which is analyzed and processed to produce failed feedback. The wireless intelligent motion correction system can find out the defects the pedaling force and frequency in the skating process in a timely manner and avoid irreparable losses in future training. It can also help coaches to formulate targeted training methods and tactics which play an important role in improving athletes' sports performance and competitive level.

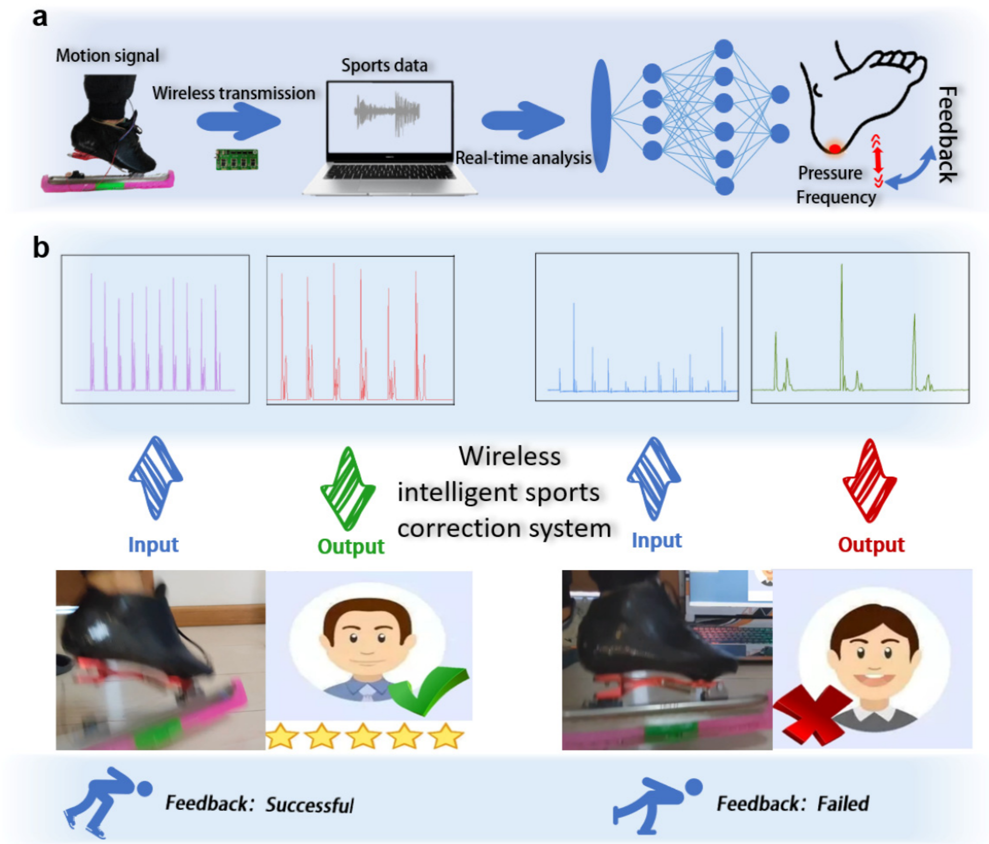

Figure 5. Application of the LPS-TENG in a wireless intelligent motion correction system. (**a**) Workflow of the wireless intelligent motion correction system. (**b**) The specific process of the wireless intelligent motion correction system.

4. Conclusions

In summary, we have made a lightweight, portable and self-powered TENG (LPS-TENG), which is mainly used to monitor the frequency and force of athletes' pedaling during skating. It uses PTFE and nylon as friction layers and copper foil as electrodes, and the substrate is made using 3D-printing technology. The LPS-TENG converts the mechanical motion of human body in to electrical signals through the working mechanism of contact–separation. The frequency and force of pedaling are important factors that affect athletes' performance. Coaches can analyze the dynamic information of each skating stage through electrical signals of pedaling frequency and pedaling force. This can help coaches to formulate correct training methods, optimize skaters' skating skills and thus improve athletes' sports performance and competitive level. Moreover, in order to make the sports data of athletes more intuitive to be mastered by coaches, we designed a wireless intelligent motion correction system, including the LPS-TENG, AD module and back-end computer. The combination of the sensors and AD module accomplishes the real-time monitoring and wireless transmission of motion data. The back-end computer makes the motion data more intuitive. The wireless intelligent motion correction system can clearly analyze the changes in different frequencies and forces in the skating process and give successful or failed feedback according to the electronic signals of frequencies and forces. This system can provide a more intuitive reference for coaches to judge athletes' sports state. This work provides a new idea for monitoring skaters' sports techniques, promotes the application of force sensors in sports monitoring and plays a positive role in promoting the development of intelligent assisted-training systems and building sports big data.

Supplementary Materials: The following supporting information can be downloaded at: https://www.mdpi.com/article/10.3390/electronics12020320/s1. Figure S1: The actual diagram of AD module; Figure S2: The circuit diagram of AD module; Figure S3: Output voltage and linear relationship of LPS-TENG under the same force and different frequencies; Figure S4: Output voltage and linear relationship of LPS-TENG under the same frequency and different forces; Video S2: Different feedback results of wireless intelligent motion correction system.

Author Contributions: Conceptualization, Z.L. and Y.M.; methodology, D.L. and Y.Z. (Yaotian Zhang); software, X.Y. and B.L.; writing—original draft preparation, Y.W., Z.L. and Y.Z. (Yongsheng Zhu); writing—review and editing, Y.W., Z.L. and Y.Z. (Yongsheng Zhu); supervision, J.Z., Y.M. and S.Z. All authors have read and agreed to the published version of the manuscript.

Funding: This research was funded by Project Plan Assignment of Heilongjiang Natural Science Foundation, grant number LH2021C056. Practice and research on digital monitoring of high-level snow and ice projects in China, grant number 2022YFF11068.

Data Availability Statement: The data presented in this study are available on request from the corresponding author.

Acknowledgments: The authors would like to thank the collaboration of all volunteers who participated in data collection.

Conflicts of Interest: The authors declare no conflict of interest. The funders had no role in the design of the study, in the collection, analyses, or interpretation of data, in the writing of the manuscript or in the decision to publish the results.

References

1. Wu, L.M.; Feng, H.T. The Deep Integration of China's Regional Ice-Snow Industry and Ecocultural Tourism under the Background of Beijing Winter Olympic Games: Taking Hunan as an Example. *J. Environ. Public Health* **2022**, *2022*, 6736709.
2. Stuart, A.; Cochrane-Snyman, K.C. Strength Training and Development in Competitive Speed Skating. *Strength Cond. J.* **2022**, *44*, 1–10. [CrossRef]
3. Asfandiyarov, D.B.; Titlov, A.Y. Training of Young Speed Skaters and the Analysis of Multi-Year Performance. *Hum. Sport Med.* **2021**, *21*, 93–100.
4. Moon, Y.; Song, J.; Kwon, K.; Kwon, O.; Kim, M.; Yoon, S.H.; Byun, Y.; Sa, A.N. Development of a Functional Speed Skating Uniform through Aerodynamic Analysis on Knit Textiles and Uniforms. *J. Eng. Fiber Fabr.* **2016**, *11*, 64–75. [CrossRef]
5. Zhang, J.Y.; Xu, Q.S.; Gan, Y.Y.; Sun, F.X.; Sun, Z.A. Lightweight Sensitive Triboelectric Nanogenerator Sensor for Monitoring Loop Drive Technology in Table Tennis Training. *Electronics* **2022**, *11*, 3212. [CrossRef]
6. Wu, W.L.; Hsu, H.T.; Chu, I.H.; Tsai, F.H.; Liang, J.M. Selected plantar pressure characteristics associated with the skating performance of national in-line speed skaters. *Sport Biomech.* **2017**, *16*, 210–219. [CrossRef]
7. Lu, Z.; Jia, C.J.; Yang, X.; Zhu, Y.S.; Sun, F.X.; Zhao, T.M.; Zhang, S.W.; Mao, Y.P. A Flexible TENG Based on Micro-Structure Film for Speed Skating Techniques Monitoring and Biomechanical Energy Harvesting. *Nanomaterials* **2022**, *12*, 1576. [CrossRef]
8. Lu, Z.; Zhu, Y.S.; Jia, C.J.; Zhao, T.M.; Bian, M.Y.; Jia, C.F.; Zhang, Y.Q.; Mao, Y.P. A Self-Powered Portable Flexible Sensor of Monitoring Speed Skating Techniques. *Biosensensors* **2021**, *11*, 108. [CrossRef]
9. Wang, A.R.; Yang, L.; Wen, W.M.; Zhang, S.; Hao, D.M.; Khalid, S.G.; Zheng, D.C. Quantification of radial arterial pulse characteristics change during exercise and recovery. *J. Physiol. Sci.* **2018**, *68*, 113–120. [CrossRef]
10. Roslan, M.F.; Ahmad, A. Internet of Things (IoT)-based Solution for Real-time Monitoring System in High Jump Sport. *Int. J. Integr. Eng.* **2019**, *11*, 197–205.

11. Knobbe, A.; Orie, J.; Hofman, N.; van der Burgh, B.; Cachucho, R. Sports analytics for professional speed skating. *Data Min. Knowl. Disc.* **2017**, *31*, 1872–1902. [CrossRef]
12. Gai, L.Z.; Wang, F.T.; Zhou, F.Z. A Stretchable Triboelectric Nanogenerator Integrated Ion Coagulation Electrode for Cheerleading Monitoring. *J. Electron. Mater.* **2022**, *51*, 7182–7189. [CrossRef]
13. Sun, F.X.; Zhu, Y.S.; Jia, C.J.; Ouyang, B.W.; Zhao, T.M.; Li, C.X.; Ba, N.; Li, X.; Chen, S.; Che, T.T.; et al. A Flexible Lightweight Triboelectric Nanogenerator for Protector and Scoring System in Taekwondo Competition Monitoring. *Electronics* **2022**, *11*, 1306. [CrossRef]
14. Ma, X.F.; Liu, X.; Li, X.X.; Ma, Y.F. Light-Weight, Self-Powered Sensor Based on Triboelectric Nanogenerator for Big Data Analytics in Sports. *Electronics* **2021**, *10*, 2322. [CrossRef]
15. Bukhari, M.U.; Khan, A.; Maqbool, K.Q.; Arshad, A.; Riaz, K.; Bermak, A. Waste to energy: Facile, low-cost and environment-friendly triboelectric nanogenerators using recycled plastic and electronic wastes for self-powered portable electronics. *Energy Rep.* **2022**, *8*, 1687–1695. [CrossRef]
16. Sun, P.; Cai, N.X.; Zhong, X.D.; Zhao, X.J.; Zhang, L.; Jiang, S.H. Facile monitoring for human motion on fireground by using MiEs-TENG sensor. *Nano Energy* **2021**, *89*, 106492. [CrossRef]
17. Jiang, M.; Lu, Y.; Zhu, Z.Y.; Jia, W.Z. Advances in Smart Sensing and Medical Electronics by Self-Powered Sensors Based on Triboelectric Nanogenerators. *Micromachines* **2021**, *12*, 698. [CrossRef]
18. Xu, G.P.; Zheng, Y.B.; Feng, Y.G.; Ma, S.C.; Luo, N.; Feng, M.; Chen, S.G.; Wang, D. A triboelectric/electromagnetic hybrid generator for efficient wind energy collection and power supply for electronic devices. *Sci. China Technol. Sci.* **2021**, *64*, 2003–2011. [CrossRef]
19. Sun, W.J.; Li, B.; Zhang, F.; Fang, C.L.; Lu, Y.J.; Gao, X.; Cao, C.J.; Chen, G.M.; Zhang, C.; Wang, Z.L. TENG-Bot: Triboelectric nanogenerator powered soft robot made of uni-directional dielectric elastomer. *Nano Energy* **2021**, *85*, 106012. [CrossRef]
20. Zheng, Q.; Zou, Y.; Zhang, Y.L.; Liu, Z.; Shi, B.J.; Wang, X.X.; Jin, Y.M.; Ouyang, H.; Li, Z.; Wang, Z.L. Biodegradable triboelectric nanogenerator as a life-time designed implantable power source. *Sci. Adv.* **2016**, *2*, e1501478. [CrossRef]
21. Garcia, A.J.L.; Jalabert, T.; Pusty, M.; Defoor, V.; Mescot, X.; Montanino, M.; Sico, G.; Loffredo, F.; Villani, F.; Nenna, G.; et al. Size and Semiconducting Effects on the Piezoelectric Performances of ZnO Nanowires Grown onto Gravure-Printed Seed Layers on Flexible Substrates. *Nanoenergy Adv.* **2022**, *2*, 197–209. [CrossRef]
22. Garcia, A.J.L.; Sico, G.; Montanino, M.; Defoor, V.; Pusty, M.; Mescot, X.; Loffredo, F.; Villani, F.; Nenna, G.; Ardila, G. Low-Temperature Growth of ZnO Nanowires from Gravure-Printed ZnO Nanoparticle Seed Layers for Flexible Piezoelectric Devices. *Nanomaterials* **2021**, *11*, 1430. [CrossRef]
23. Luo, J.J.; Gao, W.C.; Wang, Z.L. The Triboelectric Nanogenerator as an Innovative Technology toward Intelligent Sports. *Adv. Mater.* **2021**, *33*, 2004178. [CrossRef]
24. Wu, Y.S.; Liu, Q.; Cao, J.; Li, K.; Cheng, G.G.; Zhang, Z.Q.; Ding, J.N.; Jiang, S.Y. Design and output performance of vibration energy harvesting triboelectric nanogenerator. *Acta Phys. Sin.* **2019**, *68*, 190201. [CrossRef]
25. Liu, G.L.; Chen, J.; Guo, H.Y.; Lai, M.H.; Pu, X.J.; Wang, X.; Hu, C.G. Triboelectric nanogenerator based on magnetically induced retractable spring steel tapes for efficient energy harvesting of large amplitude motion. *Nano Res.* **2018**, *11*, 633–641. [CrossRef]
26. Yang, P.; Wang, P.F.; Diao, D.F. Graphene Nanosheets Enhanced Triboelectric Output Performances of PTFE Films. *Acs. Appl. Electron. Mater.* **2022**, *4*, 2839–2850. [CrossRef]
27. Yang, W.Q.; Chen, J.; Zhu, G.; Wen, X.N.; Bai, P.; Su, Y.J.; Lin, Y.; Wang, Z.L. Harvesting vibration energy by a triple-cantilever based triboelectric nanogenerator. *Nano Res.* **2013**, *6*, 880–886. [CrossRef]
28. Sun, Y.S.; Zhang, J.J.; Li, C.Y.; Yang, J.; Li, H.; Jiang, T.; Chen, B.D. Double-Network Hydrogel for Stretchable Triboelectric Nanogenerator and Integrated Electroluminescent Skin with Self-Powered Rapid Visual Sensing. *Electronics* **2022**, *11*, 1928. [CrossRef]
29. Liu, C.R.; Li, J.Q.; Che, L.F.; Chen, S.Q.; Wang, Z.K.; Zhou, X.F. Toward large-scale fabrication of triboelectric nanogenerator (TENG) with silk-fibroin patches film via spray-coating process. *Nano Energy* **2017**, *41*, 359–366. [CrossRef]
30. Wu, Z.P.; Chen, J.; Boukhvalov, D.W.; Luo, Z.Y.; Zhu, L.J.; Shi, Y.J. A new triboelectric nanogenerator with excellent electric breakdown self-healing performance. *Nano Energy* **2021**, *85*, 105990. [CrossRef]
31. Zhang, H.; Zhang, D.Z.; Wang, D.Y.; Xu, Z.Y.; Yang, Y.; Zhang, B. Flexible single-electrode triboelectric nanogenerator with MWCNT/PDMS composite film for environmental energy harvesting and human motion monitoring. *Rare Met.* **2022**, *41*, 3117–3128. [CrossRef]
32. Chu, W.C.C.; Shih, C.; Chou, W.Y.; Ahamed, S.I.; Hsiung, P.A. Artificial Intelligence of Things in Sports Science: Weight Training as an Example. *Computers* **2019**, *52*, 52–61. [CrossRef]
33. Li, W.J.; Lu, L.Q.; Kottapalli, A.G.P.; Pei, Y.T. Bioinspired sweat-resistant wearable triboelectric nanogenerator for movement monitoring during exercise. *Nano Energy* **2022**, *95*, 107018. [CrossRef]
34. Xi, Y.; Guo, H.Y.; Zi, Y.L.; Li, X.G.; Wang, J.; Deng, J.N.; Li, S.M.; Hu, C.G.; Cao, X.; Wang, Z.L. Multifunctional TENG for Blue Energy Scavenging and Self-Powered Wind-Speed Sensor. *Adv. Energy Mater.* **2017**, *7*, 1602397. [CrossRef]
35. Wang, Z.; Gao, W.Y. A wave structure triboelectric nanogenerator for race walking motion sensing. *Mater. Technol.* **2022**, *37*, 2637–2643. [CrossRef]
36. Kwon, D.H.; Kwon, J.H.; Jeong, J.; Lee, Y.; Biswas, S.; Lee, D.W.; Lee, S.; Bae, J.H.; Kim, H. Textile Triboelectric Nanogenerators with Diverse 3D-Spacer Fabrics for Improved Output Voltage. *Electronics* **2021**, *10*, 937. [CrossRef]

37. Zhu, Y.S.; Sun, F.X.; Jia, C.J.; Huang, C.R.; Wang, K.; Li, Y.; Chou, L.P.; Mao, Y.P. A 3D Printing Triboelectric Sensor for Gait Analysis and Virtual Control Based on Human-Computer Interaction and the Internet of Things. *Sustainability* **2022**, *14*, 10875. [CrossRef]
38. Lin, Z.M.; Wu, Z.Y.; Zhang, B.B.; Wang, Y.C.; Guo, H.Y.; Liu, G.L.; Chen, C.Y.; Chen, Y.L.; Yang, J.; Wang, Z.L. A Triboelectric Nanogenerator-Based Smart Insole for Multifunctional Gait Monitoring. *Adv. Mater. Technol.* **2019**, *4*, 1800360. [CrossRef]
39. Yang, P.; Shi, Y.X.; Li, S.Y.; Tao, X.L.; Liu, Z.Q.; Wang, X.L.; Wang, Z.L.; Chen, X.Y. Monitoring the Degree of Comfort of Shoes In-Motion Using Triboelectric Pressure Sensors with an Ultrawide Detection Range. *Acs. Nano* **2022**, *16*, 4654–4665. [CrossRef]
40. Varghese, H.; Hakkeem, H.M.A.; Farman, M.; Thouti, E.; Pillai, S.; Chandran, A. Self-powered flexible triboelectric touch sensor based on micro-pyramidal PDMS films and cellulose acetate nanofibers. *Results Eng.* **2022**, *16*, 100550. [CrossRef]
41. Wei, X.L.; Wang, B.C.; Wu, Z.Y.; Wang, Z.L. An Open-Environment Tactile Sensing System: Toward Simple and Efficient Material Identification. *Adv. Mater.* **2022**, *34*, 2203073. [CrossRef] [PubMed]
42. Varghese, S.S.; Varghese, S.H.; Swaminathan, S.; Singh, K.K.; Mittal, V. Two-Dimensional Materials for Sensing: Graphene and Beyond. *Electronics* **2015**, *4*, 651–687. [CrossRef]
43. Wang, Y.F.; Jin, X.; Wang, W.Y.; Niu, J.R.; Zhu, Z.T.; Lin, T. Efficient Triboelectric Nanogenerator (TENG) Output Management for Improving Charge Density and Reducing Charge Loss. *Acs. Appl. Electron. Mater.* **2021**, *3*, 532–549. [CrossRef]
44. Zhou, Y.M.; Tao, X.J.; Wang, Z.Q.; An, M.; Qi, K.; Ou, K.K.; He, J.X.; Wang, R.W.; Chen, X.G.; Dai, Z. Electret-Doped Polarized Nanofiber Triboelectric Nanogenerator with Enhanced Electrical Output Performance Based on a Micro-Waveform Structure. *Acs. Appl. Electron. Mater.* **2022**, *4*, 2473–2480. [CrossRef]
45. Liu, R.; Li, M.P. A textile-based triboelectric nanogenerator for long jump monitoring. *Mater. Technol.* **2022**, *37*, 2360–2367. [CrossRef]
46. Zhou, Y.M.; Shen, H. Wireless Sensor Network Technology-Based Design and Realization of Intelligent Tennis Sports System. *Wirel. Commun. Mob. Com.* **2022**, *2022*, 3260000. [CrossRef]
47. Gottschall, J.S.; Palmer, B.M. The acute effects of prior cycling cadence on running performance and kinematics. *Med. Sci. Sport Exerc.* **2002**, *34*, 1518–1522. [CrossRef] [PubMed]